

## Chapter 1

# Nanoparticle Metal Oxides for Chlorocarbon and Organophosphonate Remediation

Olga B. Koper\*, Shyamala Rajagopalan\*, Slawomir Winecki\*  
and Kenneth J. Klabunde\*,<sup>†</sup>

*\*NanoScale Corporation, Inc., Manhattan, KS, USA  
and*

*<sup>†</sup>Kansas State University, Manhattan, KS, USA*

### Introduction

The nanotechnology revolution affects many areas of science including chemistry and chemical engineering. Although nanotechnology advances in electronic or in manufacturing of “nano machines” are rather recent developments, nanoscale chemical structures are much older. Materials known and widely used over the past several decades, such as high surface area carbons, porous inorganic metal oxides, and highly dispersed supported catalysts all fall into the category of nanostructures. Although a few decades-old publications describing these materials rarely used the word “nano”, they deserve proper credit for providing the foundation of current advances in nano-chemistry.

Since approximately the 1970s, enormous advances in the synthesis, characterization, and understanding of high surface area materials have taken place and this period can be justifiably described as the nanoscale revolution. Development and commercial use of methods like sol-gel synthesis, chemical vapor deposition, and laser induced sputtering allowed for manufacturing of countless new nanomaterials both at laboratory- and commercial-scale. Traditional chemical manufacturing methods, used in catalyst synthesis or in production of porous sorbents, were gradually improved by systematic development of methodologies, as well as quality control measures. In addition, characterization of nanostructures was revolutionized by an availability of new instruments. Various high-resolution

microscopic tools were developed and became available commercially. For the first time, pictures of nano-objects became easily obtainable. Today, they appear not only in scientific literature but also in popular magazines and textbooks. Measurement of specific surface area, once a tedious and lengthy laboratory procedure, is done today routinely using automatic yet affordable instruments. Numerous companies develop, manufacture and sell scientific equipment specifically for nano-research, which resulted in more instruments being available and at reduced costs. The understanding of nanostructures grows at a phenomenal rate due to efforts of countless research groups, academic institutions and commercial entities. Since approximately 1990, nano-science has been recognized as a distinct field of study with tremendous potential. As a result, nanotechnology research has proliferated, scientific journals dedicated to nano-science were created, nanotechnology research centers were established, and universities have opened faculty positions related to nano-research. These developments were, and continue to be, heavily supported by the federal and local governments in the form of research grants and other funding opportunities. Private organizations, including all major chemical manufacturers, started robust nanotechnology programs and investments.

This chapter is intended as a brief description of the technology and products developed in the laboratories of one of the authors (Kenneth J. Klabunde) at Kansas State University, Manhattan, KS; and by NanoScale<sup>®</sup> Corporation, Manhattan, KS. The description will start with a reminder of a few technical concepts related to all nanoscale materials intended for chemical uses.

Nano-materials have large specific surface areas and a large fraction of atoms are available for chemical reaction. Figure 1 presents a high-resolution transmission electron microscopy (TEM) image of aerogel-prepared nanocrystalline MgO. The image demonstrates the nano-morphology of this material with rectangular crystals, 2–4 nm in size, a length-scale that is only an order of magnitude larger than distances between atoms of this oxide. It is apparent that significant fractions of atoms are located on crystallite surfaces as well as on edges and corners. These atoms/ions are partially unsaturated (coordination less than 6) and can readily interact with chemical species that come in contact with the nanocrystallites. Such interaction can be a physical adsorption, if caused by van der Waals attraction, or a chemical reaction if chemical bonds are formed or modified. Simple estimations presented in Figure 2 demonstrate that reduction of size of nanocrystallites results in a sharp increase of specific surface areas, as well as fractions of atoms located on surfaces, edges and corners. For instance, a material with 2 nm crystallites has more than half of the atoms located on their surface, approximately 10% of atoms/ions

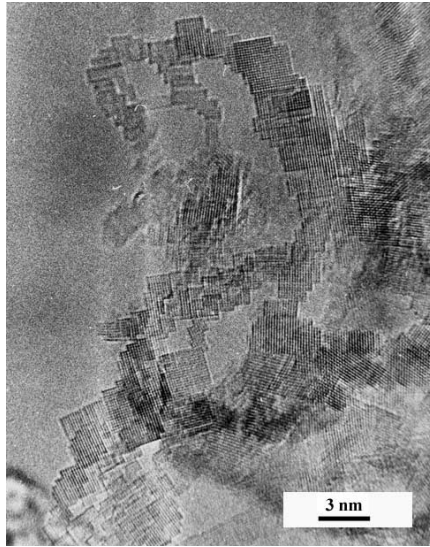


Figure 1. High-resolution Transmission Electron Microscopy (TEM) image of nanocrystalline MgO.

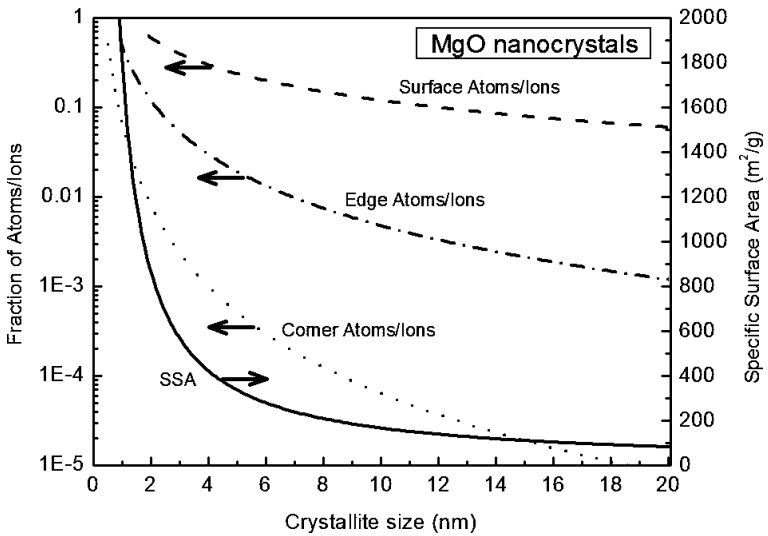


Figure 2. Specific surface area and fractions of atoms/ions located on surface, edges and corners of nanocrystalline magnesium oxide.

are on edges, 1% of atoms/ions are placed on corners, and with specific surface area approaching  $1,000 \text{ m}^2/\text{g}$ . It is important to recognize that the trends demonstrated in Figure 2 apply to all porous nanocrystalline and amorphous solids; and are the basis of the unique reactivity of nanocrystalline materials in chemical applications. Amorphous materials can be viewed as a limiting case of nanocrystalline materials with the crystallite size approaching inter-atomic distances.

One of the major important features of nanocrystalline materials is related to the size of pores between crystallites. It is apparent from Figure 1 that most pores between crystallites are similar in size as the crystallites themselves; therefore, nanocrystalline materials have a large fraction of pores below 10 nm that are traditionally described in literature as micropores. Fluids, and particularly gases, behave differently inside of micropores as compared to normal conditions. The first difference involves Knudsen diffusivity; conditions where collisions between fluid molecules are less frequent than collisions between fluid and pore-walls, and this is likely to dominate pores below 10–100 nm size-range, as shown in Figure 3. This mode of diffusivity is significantly slower than regular diffusivity for an unbound gas and will result in slower mass transfer within nanocrystalline materials. Gas diffusivities in micropores may be two- to four-orders of magnitude smaller

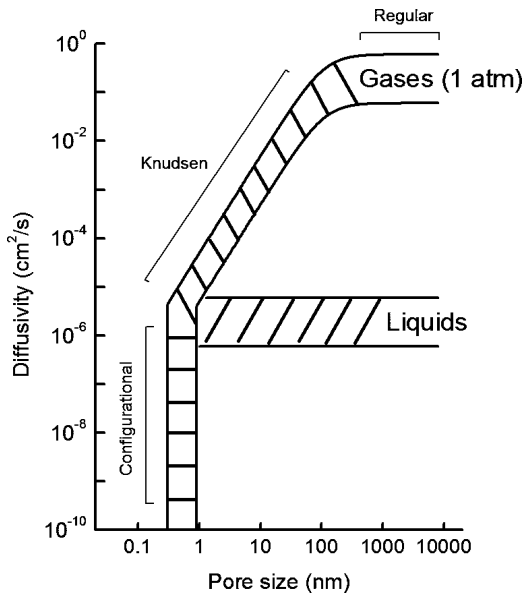


Figure 3. Influence of the pore size on diffusivities of gases and liquids.

than diffusivities known for gases and may approach liquid diffusivities. The reduced diffusivities need to be taken into account in the engineering design. The second consequence of the micropores is the possibility of capillary condensation of vapors and gases and enhanced adsorption by nanocrystalline materials. The capillary condensation phenomenon is traditionally described by the Kelvin equation that relates reduction of the equilibrium vapor pressure inside of pores to pore-size and physical properties of a chemical. The reduction of the equilibrium vapor pressures for several common substances, predicted by the Kelvin equation, is shown in Figure 4. It is apparent that the equilibrium pressure reduction and capillary condensation effects become pronounced for micropores. On the other hand, nanocrystalline materials, when aggregated into microstructures or pellets, also possess numerous mesopores. Thus, both micropores and mesopores need to be considered in describing the behavior of this new class of materials (Table 1).

Physical properties of select nanocrystalline metal oxides (NanoActive<sup>®</sup> materials) manufactured by NanoScale are shown in Table 1. The surface areas range from 20 to over 600 m<sup>2</sup>/g for the NanoActive Plus metal oxides. Figure 5 shows the powder X-Ray Diffraction (XRD) spectra of commercial MgO, NanoActive MgO and NanoActive MgO Plus. The Plus material has the broadest peaks indicating the smallest crystallites. These nanometer-sized small crystallites, due to the high surface reactivity, aggregate into

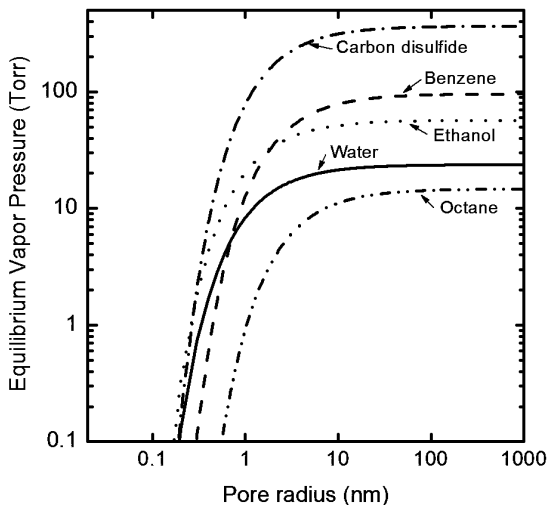


Figure 4. Reduction of the equilibrium vapor pressures inside cylindrical pores for several common substances as predicted by the Kelvin equation.

Table 1. Physical properties of nanocrystalline metal oxides.

NanoActive Material	Powder Appearance	Surface Area ( $\text{m}^2\text{g}^{-1}$ )	Crystallite Size (nm)	Average Pore-Diameter ( $\text{\AA}$ )	Mean Particle-Size ( $\mu\text{m}$ )
MgO Plus	White	$\geq 600$	$\leq 4$	30	12
MgO	White	$\geq 230$	$\leq 8$	50	3.3
CaO Plus	White	$\geq 90$	$\leq 20$	110	4
CaO	White	$\geq 20$	$\leq 40$	165	4
Al <sub>2</sub> O <sub>3</sub> Plus	White	$\geq 550$	Amorphous	110	5
Al <sub>2</sub> O <sub>3</sub>	White	$\geq 275$	Amorphous	28	1.5
CuO	Black	$\geq 65$	$\leq 8$	85	6
ZnO	Off-White	$\geq 70$	$\leq 10$	170	4
TiO <sub>2</sub>	White	$\geq 500$	Amorphous	32	5
CeO <sub>2</sub>	Yellow	$\geq 50$	$\leq 7$	70	9.5



Figure 5. Powder X-ray Diffraction spectra of commercial MgO, NanoActive MgO, and NanoActive MgO Plus.

larger particles (micron size) that preserve the high chemical reactivity, yet are much easier to handle.

## **Environmental Applications of NanoActive Materials**

There are many areas where nanocrystalline materials can be used, but the environmental applications of these materials are particularly significant. Air and water pollution continues to be a challenge in all parts of the World. In many instances, the pollution control technology is limited by poor performance and/or high costs of existing sorbent materials; and considerable research activity is directed towards development of new sorbents. The following list gives a few examples of such cases:

- Control of chemical spills and accidental releases of harmful chemicals at various locations and settings: Accidental chemical releases are common occurrences in laboratories, industrial locations and all places where chemicals are used. Spills and accidental releases often result in environmental contaminations. NanoScale developed a specialized, safe sorbent formulation, FAST-ACT<sup>®</sup> (First Applied Sorbent Treatment — Against Chemical Threats), a powder capable of safe spill treatment and environmentally responsible disposal.
- Protection from chemical hazards: Nanocrystalline metal oxides can be incorporated into protective textiles or skin-creams to provide additional protection from chemical and biological hazards. The toxic agents are destroyed on nanoparticles, eliminating the threat of off-gassing and secondary contamination.
- Indoor air quality-control in buildings and vehicles: Currently, various air filtration technologies are available commercially; including particulate filters, electrostatic precipitators, and activated-carbon filters. There remains a large group of high volatility chemicals that cannot be effectively controlled by these approaches. Attempts to develop more effective sorbents or catalysts for these pollutants are on-going.
- Removal of elemental and oxidized mercury from combustion gases generated by electrical utilities using coal as a source of energy: Recent regulations enacted by the U.S. Environmental Protection Agency (EPA) spurred widespread development of new mercury sorbents, including activated-carbons and metal oxides.
- Control of arsenic, perchlorate, and methyl-*t*-butyl ether (MTBE) in drinking water: The presence of these compounds in water causes serious health concerns; and has resulted in mandatory maximum contaminant levels (MCL) for arsenic and may trigger new EPA regulations.

Development of new sorbents for economical and efficient removal of these pollutants is an active area of research.

The above applications, as well as numerous others, can benefit from the use of nanocrystalline sorbents owing to enhancement in reaction kinetics, increased removal capacities, and permanent destruction of harmful chemicals.

Nanocrystalline materials exhibit a wide array of unusual properties, and can be considered as new materials that bridge molecular and condensed matter.<sup>1</sup> One of the unusual features is enhanced surface chemical reactivity (normalized for surface area) toward incoming adsorbates.<sup>2</sup> For example, nanocrystalline MgO, CaO, TiO<sub>2</sub> and Al<sub>2</sub>O<sub>3</sub> adsorb polar organics such as aldehydes and ketones in very high capacities, and substantially outperform the activated-carbon samples that are normally utilized for such purposes.<sup>3</sup> Many years of research at Kansas State University, and later at NanoScale, have clearly established the destructive adsorption capability of nanoparticles towards many hazardous substances, including chlorocarbons, acid gases, common air-pollutants, dimethyl methylphosphonate (DMMP), paraoxon, 2-chloroethylethyl sulfide (2-CEES), and even military agents such as GD, VX, and HD.<sup>4-9</sup> The enhanced chemical reactivity suggests a two-step decomposition mechanism of the adsorbates on nanoparticles (first step — adsorption of toxic agent on the surface by means of physisorption, followed by the second step — chemical decomposition). This two-step mechanism substantially enhances the detoxification abilities of nanoparticles because it makes the decomposition less dependent on the rate (speed) of chemical reaction. The rate of chemical reaction depends on the agent-nanoparticle combination; therefore, for some agents the rate may be quite low. In addition, the reaction rate strongly decreases at lower temperatures. For these reasons, any detoxification method that relies only on chemical reactivity would not work for many toxic agents and would not be effective at low temperatures. Reactive nanoparticles do not have this drawback because the surface adsorption sites remain active even at very low temperatures. In fact, the physisorption of the potential toxic agents is enhanced at low temperatures. In this way, the toxins are trapped and eventually undergo “destructive adsorption.”

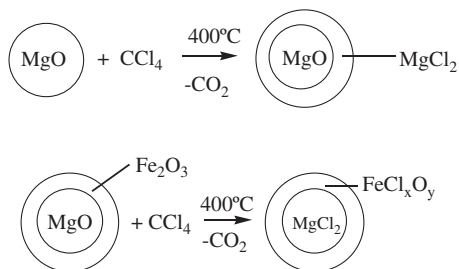
## **Destructive Adsorption of Hazardous Chemicals by Nanocrystalline Metal Oxides**

A wide variety of chlorinated compounds such as cleaning-solvents, plasticizers, lubricants, and refrigerants are used by society in many beneficial functions. While some of these chlorinated compounds are being replaced

by less harmful chemicals, many continue to be used because of the lack of suitable replacements or as a result of economic considerations. Therefore, considerable interest exists in developing methods for the safe disposal of chlorinated and other problematic wastes. It has been shown that nanocrystalline metal oxides are particularly effective decontaminants for several classes of environmentally problematic compounds at elevated temperatures; enabling complete destruction of these compounds at considerably lower temperatures than that required for incineration.<sup>10</sup>

Koper *et al.*,<sup>11–15</sup> have examined the reaction of aerogel-prepared CaO with carbon tetrachloride and other chlorinated hydrocarbons. The primary carbon-containing product was CO<sub>2</sub>, with the CaO converted to CaCl<sub>2</sub>. Conventionally-prepared CaO, however, produced little CO<sub>2</sub>. A three-step mechanism was proposed. Initially, CO<sub>2</sub> and CaCl<sub>2</sub> are produced from metathesis of CaO and CCl<sub>4</sub>; CO<sub>2</sub> then combines with CaO in a second step to yield CaCO<sub>3</sub>; finally, metathesis of CaCO<sub>3</sub> and CCl<sub>4</sub> generates CaCl<sub>2</sub> and CO<sub>2</sub>. Phosgene, COCl<sub>2</sub>, is an intermediate, which reacts with the remaining CaO to form calcium chloride and carbon dioxide. Low-temperature infrared studies of CCl<sub>4</sub> monolayers on CaO demonstrated that CCl<sub>x</sub> intermediates begin to form at temperatures above 113 K; at 200 K, CCl<sub>4</sub> and CCl<sub>x</sub> are no longer observed.<sup>13</sup> Although the reactions of chlorocarbons with metal oxides are often thermodynamically favorable, liquid-solid or gas-solid reactions are involved only on the surface of the metal oxide. Kinetic parameters involving ion (Cl<sup>-</sup>/O<sup>2-</sup>) migration inhibit complete reaction. Therefore, the use of ultrahigh surface area metal oxides allows reasonably high capacities for such chlorocarbon destructive adsorption processes<sup>16</sup>: Li *et al.*,<sup>17,18</sup> have studied the reactions of aerogel-prepared CaO and MgO with chlorinated aromatics at 500–900°C. Upon destruction of chlorobenzene, a biphenyl was formed as the reaction by-product. Destruction of chlorinated aromatics occurred to a much greater extent, and at significantly lower temperatures, relative to destruction in the absence of the nanoscale metal oxides. Trace toxins such as dibenzo-*p*-dioxins were not observed under any conditions when aerogel-prepared MgO was used, nor when aerogel-prepared CaO was used in the presence of oxygen in the carrier gas. However, when low surface area CaO was used in the presence of oxygen, small amounts of dibenzo-*p*-dioxins were produced. Hooker and Klabunde<sup>19</sup> have studied the reaction of iron(III) oxide with carbon tetrachloride in a fixed-bed pulse reactor, from 400 to 620°C. The main carbon-containing product was CO<sub>2</sub>; other carbon-containing products included C<sub>2</sub>Cl<sub>4</sub>, and graphite. It was found that the extent of reaction was greater than what could be accounted for by reaction only on surfaces of Fe<sub>2</sub>O<sub>3</sub>; this suggested that Fe<sub>2</sub>O<sub>3</sub> on the surface was regenerated. The apparent regeneration of Fe<sub>2</sub>O<sub>3</sub> on the surface of the particles suggested that coating other metal oxide nanoparticles with iron(III) oxide might enable more complete

utilization of the core metal oxide. Accordingly, aerogel-prepared MgO overlaid with Fe<sub>2</sub>O<sub>3</sub> (designated as [Fe<sub>2</sub>O<sub>3</sub>]MgO) was prepared, and its reactions with carbon tetrachloride were examined by Klabunde *et al.*,<sup>20</sup> Khaleel and Klabunde,<sup>21</sup> and Kim *et al.*<sup>22</sup> It was found that when [Fe<sub>2</sub>O<sub>3</sub>]MgO reacted with CCl<sub>4</sub>, nearly all of the metal oxides (MgO) were consumed, in contrast, Fe<sub>2</sub>O<sub>3</sub> treatment of conventionally-prepared MgO did not give this enhancement. Since the iron oxide coating is regenerated by the core MgO, the Fe<sub>2</sub>O<sub>3</sub> coating can be considered to be catalytic. The scheme below indicates the reaction of carbon tetrachloride with nanocrystalline MgO and iron-coated nanocrystalline MgO.



Further work, using X-ray Photoelectron Spectroscopy (XPS), showed that the best catalysts were those where Fe<sub>2</sub>O<sub>3</sub> was coated on the surface of the MgO,<sup>23</sup> and was highly dispersed (as shown by Mossbauer spectroscopy<sup>24</sup> and XRD). Simple mixtures of Fe<sub>2</sub>O<sub>3</sub> with MgO were not as effective and solid state mixtures of Fe<sub>2</sub>O<sub>3</sub>-MgO were also less effective. Indeed, a layered [Fe<sub>2</sub>O<sub>3</sub>]MgO structure worked best. Figure 6 shows the destructive adsorption of carbon tetrachloride on two forms of nanocrystalline CaO coated with iron oxide and vanadium oxide. Again, the same trends were observed, where the sol-gel-based form of the CaO exhibited higher chemical reactivity as compared to the nanocrystalline CaO (nano), whose reactivity was much higher than the commercially available CaO. Furthermore, a coating of the transition metal oxide imparted additional reactivity driving the reaction closer to its stoichiometric limit.

Other metal oxides were also found to be effective coatings for enhancing the utilization of aerogel-prepared MgO. Indeed, Fe<sub>2</sub>O<sub>3</sub> enhanced the catalytic properties of both MgO and SrO.<sup>25,26</sup> In an attempt to gain more detailed information on the chemical state of the Fe<sub>2</sub>O<sub>3</sub>/FeCl<sub>x</sub> before, during, and after CCl<sub>4</sub> reaction, a series of [Fe<sub>2</sub>O<sub>3</sub>]SrO nanocrystals and microcrystals were studied by Jiang *et al.*, using Extended X-ray Absorption Fine-Structure Spectroscopy (EXAFS).<sup>27</sup> Strontium was chosen as the base oxide because of available synchrotron energies. The results of these experiments were quite surprising. First of all, the data showed that SrO

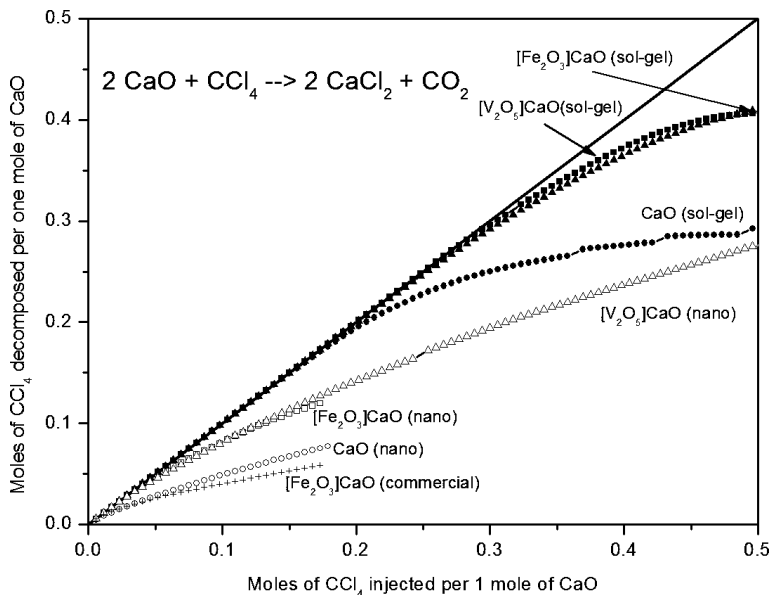


Figure 6. Decomposition ability of CaO and  $[\text{V}_2\text{O}_5]\text{CaO}$  towards  $\text{CCl}_4$ . In a stoichiometric reaction 1 model of CaO can decompose 0.5 moles of  $\text{CCl}_4$ .

itself was more reactive than CaO, which is known to be more reactive than MgO (per unit surface area, although MgO can be prepared in the highest surface area). Also, it was found that the  $\text{Cl}^-/\text{O}^{2-}$  exchange was extremely facile, and even after near stoichiometric exposure to  $\text{CCl}_4$ ,  $\text{Fe}_2\text{O}_3$  remained as  $\text{Fe}_2\text{O}_3$ . In other words, if any SrO was still available, it readily gave up its  $\text{O}^{2-}$  to  $\text{FeCl}_x$  to reform  $\text{Fe}_2\text{O}_3$ .<sup>27</sup>

Besides  $\text{CCl}_4$ , other chlorocarbons have been examined. The decomposition of  $\text{CCl}_3\text{F}$  by several vanadium oxides- and vanadium oxide-coated aerogel-prepared MgO was studied by Martyanov and Klabunde.<sup>28</sup>  $\text{V}_2\text{O}_3$  was consumed in the reaction, with some vanadium-halogen species being produced. Capture of the volatile vanadium-halogen species by MgO was thought to be responsible for the catalytic effect of the vanadium compounds on MgO. Furthermore,  $\text{Fe}_2\text{O}_3$  exchange catalysis was found to work well for 1,3-dichlorobenzene, but not for trichloroethylene. Obviously, the catalytic effect of transition metal oxides depends a great deal on the intimate mechanistic details that are, of course, different for each chlorocarbon under study. Interestingly, this type of catalytic action is not restricted to  $\text{O}^{2-}/\text{Cl}^-$  exchange, but also operates in  $\text{O}^{2-}/\text{SO}_x^{n-}$ , and  $\text{O}^{2-}/\text{PO}_x^{n-}$  systems as well.<sup>24</sup>

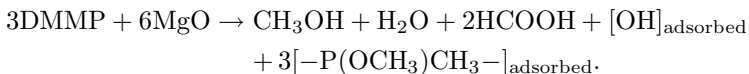
Chemical decomposition of dimethyl methyl phosphonate (DMMP), trimethyl phosphate (TMP), and triethyl phosphate (TEP) on MgO was studied by Li *et al.*<sup>29–31</sup> The agents were allowed to adsorb on the MgO samples both in vacuum environment and in a helium stream. Substantial amounts of strongly chemisorbed agents were observed at room and at elevated temperatures (500°C). At low temperatures, the main volatile reaction products were formic acid, water, alcohols, and alkenes. At higher temperatures CO, CH<sub>4</sub>, and water predominated. Phosphorous-containing products remained immobilized at all temperatures. Interestingly, addition of water enhanced decomposition abilities of nanocrystalline MgO.

Detailed studies using infrared photoacoustic spectroscopy and isotope-labeling confirmed that the chemisorption occurs through the P=O bond destruction. For instance, nanocrystalline MgO is able to hydrogen bond with DMMP at room temperature; with hydrolysis of DMMP occurring to produce surface bound species as shown below.



Further studies on the decomposition of phosphonate esters (RO)<sub>2</sub>IP=O identified two important reactions, nucleophilic substitution at P and nucleophilic substitution at the alkyl carbon of an alkoxy group.<sup>32</sup> Treatment of DMMP with MgO yielded formic acid (HCOOH) as the major volatile product; other volatile products included methanol (CH<sub>3</sub>OH), dimethyl ether (CH<sub>3</sub>OCH<sub>3</sub>), and ethane (CH<sub>3</sub>CH<sub>3</sub>). Carbon dioxide, carbon monoxide, water, hydrogen, and phosphoric acid were not observed as products. All phosphorus-containing products were immobilized on the MgO surface; elemental analysis was consistent with O<sub>solid</sub>-Mg-O-P(OMe)(Me)-O-Mg-O<sub>solid</sub>, with an O<sub>solid</sub> between the two Mg atoms. For this structure, the PO bond order of the O-P-O linkage is 1.5, i.e. the two P-O bonds share one double bond.<sup>33</sup> Proton abstraction of a β-hydrogen of an ethoxy group can lead to ethylene production, which is sometimes observed in reactions of ethyl esters.<sup>34</sup> Reactivity of nanocrystalline MgO towards a range of organophosphates (RO)<sub>3</sub>P=O, organophosphites (RO)<sub>3</sub>P, and organophosphines R<sub>3</sub>P was studied by Lin *et al.*<sup>34</sup> Phosphorous compounds were allowed to adsorb on thermally activated MgO at room temperature and at elevated temperatures reaching 175°C. Most of phosphorous compounds were adsorbed and chemically decomposed in large quantities, and in some cases the reactions were essentially stoichiometric. In the most

favorable cases, approximately one phosphorus molecule was decomposed for every two MgO molecules present in the bulk. Infrared studies performed on spent sorbents indicated that phosphates adsorb very strongly through the P=O bond (P=O bond is destroyed upon adsorption) accompanied by net electron loss from the RO groups. Phosphites adsorb through the phosphorous atom with a net electron density gain by RO groups. Phosphines adsorb less strongly through the phosphorous atom. Decomposition of the phosphorous compounds yielded volatile hydrocarbons, ethers, and alcohols. Products containing phosphorous were strongly retained by the MgO surface which prevented product desorption and release into the gas phase:



As another example of the extremely high reactivity of nanocrystalline metal oxides, ambient temperature destructive adsorption of paraoxon is illustrated. Paraoxon is an insecticide and is a suitable simulant for nerve warfare agents. Figure 7 illustrates the rate of removal of paraoxon from a pentane solution over time employing various adsorbents. The removal was monitored using UV-Vis spectroscopy and reduction of the paraoxon (265–270 nm) peak was observed over time. Nanocrystalline magnesium oxide nanoparticles achieved complete adsorption within two-minutes of

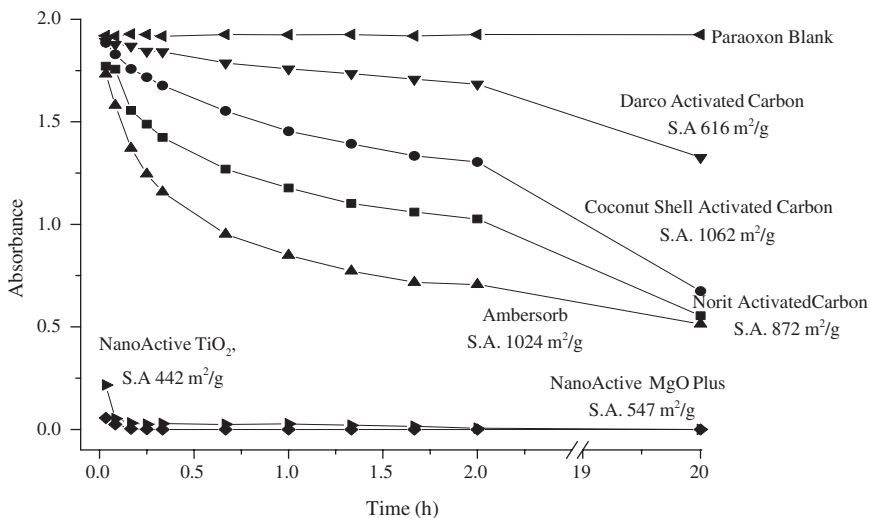
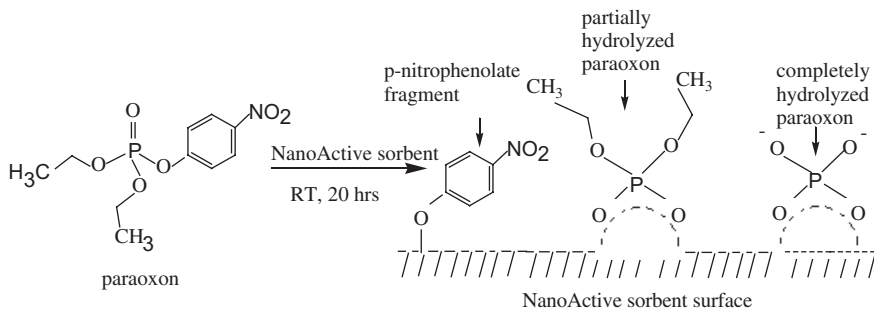


Figure 7. Rate of Adsorption of Paraoxon by various samples.

exposure to paraoxon while all the activated carbon and ion-exchange-resin (IER) samples were significantly less adsorptive and unable to adsorb paraoxon completely, even after 20 hours of exposure. In addition, with activated-carbons the agent was merely absorbed, whereas with nanoparticles it was first adsorbed onto the metal oxide surface and then decomposed into phosphate and *p*-nitrophenol:



Adsorption and hydrolysis of paraoxon is readily visible on magnesium oxide nanoparticles due to the change in color of the powder from white to bright yellow. Note that paraoxon is a light yellow, oily substance and its color does not duplicate the bright yellow observed after contact with the nanoparticles. The anion  $\text{O}_2\text{NC}_6\text{H}_4\text{O}^-$  is bright yellow, and the rapid color formation clearly shows that the anion is formed quickly on the surface of the nanoparticles. More definitive evidence for the destructive adsorptive capability of metal oxide nanoparticles comes from Nuclear Magnetic Resonance (NMR) studies.  $^{31}\text{P}$  NMR spectra of intimately mixed dry nanocrystalline metal oxide/paraoxon mixtures after 20 hours are displayed in Figure 8. Paraoxon in deuteriochloroform solvent exhibits a signal around  $-6.5$  ppm and the product derived *via* complete hydrolysis of paraoxon, namely, the phosphate ion ( $\text{PO}_4^{3-}$ ), is expected to show a signal around 0 ppm. However, it should be noted that the exact chemical shift values are sensitive to the nature of the metal oxide employed. Results from NMR studies with magnesium oxide nanoparticles over time indicate that destructive adsorption starts immediately and continues over a long period of time.

The NMR spectrum of MgO nanoparticles/paraoxon mixture contains at least four peaks. The outer peaks are due to spinning side bands. The major peak at  $\delta = 0.8$  ppm is due to completely hydrolyzed paraoxon and the peak around  $\delta = -8.2$  ppm is due to adsorbed but unhydrolyzed paraoxon. Upon close examination of the NanoActive  $\text{TiO}_2$ /paraoxon mixture spectrum, three signals were observed; a sharp peak around  $-8.4$  ppm attributed to unhydrolyzed paraoxon, a broad peak around  $-5$  ppm due

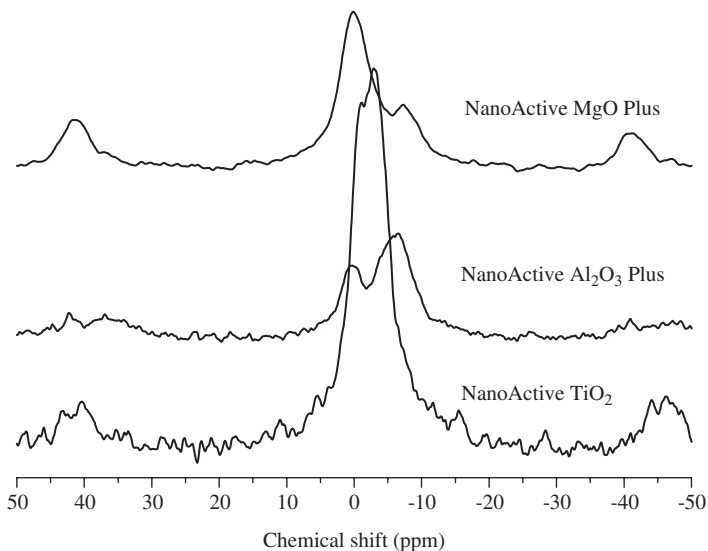


Figure 8.  $^{31}\text{P}$  NMR spectra of nanocrystalline metal oxide/Paraoxon Mixture after 20-hours.

to partially hydrolyzed paraoxon, and a shoulder peak between 0 and  $-2$  ppm was attributed to completely hydrolyzed paraoxon. The spectrum of NanoActive Aluminum Oxide Plus/paraoxon mixture displayed two major peaks. The upfield peak at  $\delta = -6.7$  ppm is attributed to partially hydrolyzed paraoxon, and the peak at 0 ppm is due to completely hydrolyzed paraoxon. In short, adsorption of paraoxon by nanoparticles occurs instantly with the destruction of the agent as an ongoing active process.

Nanocrystalline materials can be utilized in a powdered or a compacted/granulated form. Compaction of the nano crystals into pellets does not significantly degrade surface area or surface reactivity when moderate pressures are employed, ensuring that these nano structured materials can be utilized as very fine powders or as porous, reactive pellets.<sup>35</sup> As shown in Table 2, pressure can be used to control pore structure. It should be noted that below about 5,000 psi the pore structure remains relatively unchanged, and these pellets behave in adsorption processes essentially identical to the loose powders. For example, both NanoScale MgO and  $\text{Al}_2\text{O}_3$  (Figure 9) vigorously adsorb acetaldehyde with much higher rates and capacities than activated-carbon. This is the case whether the samples are loose powders or compressed pellets. As noted in Table 2, only when very high compression pressure was used, the adsorption process was hindered.

Table 2. Effects of compaction pressure on nanocrystalline MgO.

Load (psi)	Surface Area ( $\text{m}^2\text{g}^{-1}$ )	Total Pore Volume ( $\text{cm}^3\text{g}^{-1}$ )	Average Pore Diameter (nm)
0	443	0.76	6.9
5,000	434	0.57	5.3
10,000	376	0.40	4.2
20,000	249	0.17	2.7

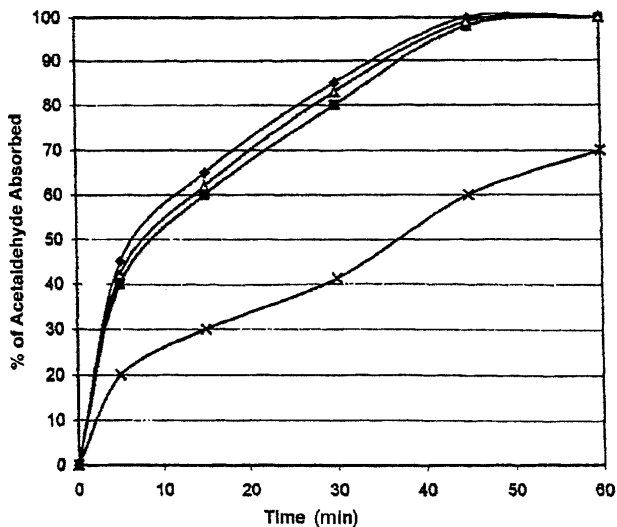


Figure 9. Rate of adsorption of acetaldehyde by nanocrystalline  $\text{Al}_2\text{O}_3$  in powder or pellet form. The following pressures were used to compact and form the pellets at room temperature:  $\blacklozenge$  = powder,  $\blacksquare$  = 5,000 psi,  $\triangle$  = 10,000 psi,  $\times$  = 20,000 psi.

The application of nanocrystalline materials as destructive adsorbents for acid gases such as HCl, HBr,  $\text{CO}_2$ ,  $\text{H}_2\text{S}$ ,  $\text{NO}_x$ , and  $\text{SO}_x$  has been investigated by Klabunde,<sup>36</sup> Stark,<sup>37</sup> and Carnes.<sup>38</sup> These materials are much more efficient than commercially-available oxides. This is seen with nanocrystalline ZnO, which reacts in a stoichiometric molar ratio of 1 mol of hydrogen sulfide to 2.4 mol of ZnO, whereas the commercial ZnO reacts in a molar ratio of 1 mol hydrogen sulfide to 32 mol ZnO. This indicates that nanoparticles are chemically more reactive at room temperatures than their commercial counterparts. For example, nanocrystalline ZnO stays at

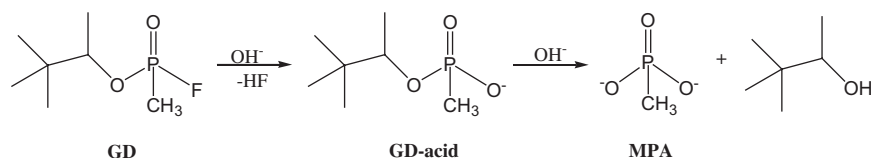
near stoichiometric ratio at room temperature, whereas the commercial ZnO does not.<sup>39</sup>

In addition to high-surface-area pure-metal-oxide nanoparticles, the development of intermingled metal oxide nanoparticles has been reported which yield special advantages.<sup>40</sup> The adsorption properties of intermingled metal oxide nanoparticles were found to be more superior than, when comparing their reactivity to, that of individual metal oxide nanoparticles and physical mixtures. For example, the nanoparticles of Al<sub>2</sub>O<sub>3</sub>/MgO mixed product have enhanced chemical reactivity over pure metal oxides of Al<sub>2</sub>O<sub>3</sub> or MgO for the adsorption of SO<sub>2</sub>. In comparison, the intermingled Al<sub>2</sub>O<sub>3</sub>/MgO showed an adsorption capacity of 6.8 molecules for SO<sub>2</sub> (of SO<sub>2</sub>/nm<sup>2</sup> adsorbed), while the nanoparticles of Al<sub>2</sub>O<sub>3</sub> and MgO was observed at 3.5 molecules and 6.0 molecules, respectively.<sup>41</sup>

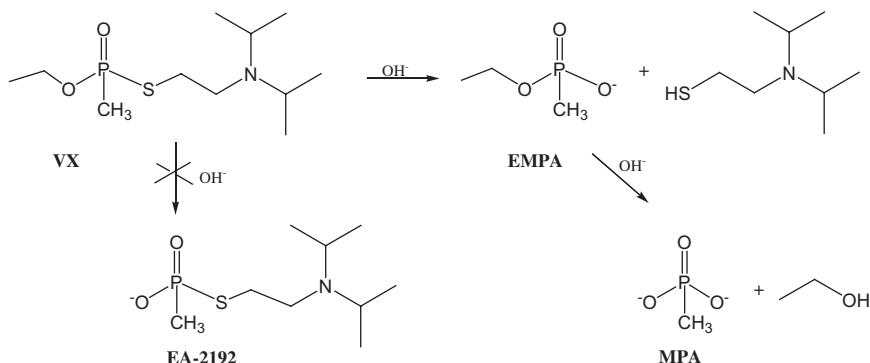
## Destructive Adsorption of Chemical Warfare Agents (CWAs) by Nanocrystalline Metal Oxides

Nanocrystalline metal oxides not only neutralize toxic industrial chemicals, but also destroy chemical warfare agents, V-, G- and H-series, through hydrolysis and/or dehydrohalogenation. The G-series tend to be volatile and highly toxic by inhalation, while the V-agents are relatively non-volatile, persistent and highly toxic by the percutaneous route. HD is an acronym for mustard gas and it belongs to the vesicant class of chemical warfare agents.

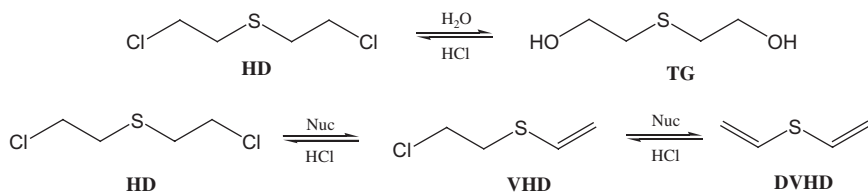
Wagner *et al.*,<sup>7-9</sup> reported that NanoScale metal oxide nanoparticles are very effective in destructive adsorption of VX, GD and HD. These studies were done at room temperature using the pure agent on a column of dry metal oxide nanoparticles. It was found that the products formed in reactions with HD were the less-toxic thioglycol (TG) and divinyl (DVHD) compounds while the nerve agents afforded the surface bound hydrolyzed species. Destruction of nerve agents (GD and VZ) and the blistering agent (HD) was studied using solid-state NMR, as well as extraction, followed by GC-MS analysis. The destruction products of GD are pinacolyl methylphosphonic acid (GD-acid) that converts to surface-bound methylphosphonic acid (MPA), and HF, which is acidic and is neutralized by the metal oxide surface as well.



The phosphonate destruction product of VX is ethyl methylphosphonic acid (EMPA) which converts into surface-bound methylphosphonic acid (MPA). It should be noted that during this reaction the toxic EA-2192 (S-(2-diisopropylamino)ethyl methylphosphonothioate) does not form, in contrast to basic VX hydrolysis in solution:



The decomposition product of HD is promoted by nucleophilic substitution on the  $\beta$ -carbon of a 2-chloroethyl group, resulting in a 2-hydroxyethyl group – thiodiglycol (TG), whereas decomposition products of HD *via* elimination are 2-chloroethyl-vinyl sulfide (CEVS) and divinyl sulfide (DVS). Both processes convert mustard to considerably less toxic compounds:



The off-gassing experiments for reactive nanoparticles after exposure to HD, GD and VX indicated, through the absence of any major chromatographable peaks, that the reaction products are either low molecular weight (less than 60 amu), small gaseous materials that were eluted with the air peaks, or compounds that are tightly bound to the nano materials.

NanoScale has developed a nanocrystalline metal-oxide-based product, FAST-ACT, that is utilized as a chemical hazard containment and neutralization system. This product can be applied manually as a dry powder for treating liquid spills, or in an aerosol form for treating toxic vapors, decontamination of vertical surfaces, or contaminated suits (Figure 10). Nanocrystalline metal oxides have low bulk density and remain suspended in the air for a prolonged period of time.



Figure 10. Decontamination of a First Responder's suit utilizing FAST-ACT.

The effectiveness of FAST-ACT has been verified against chemical warfare agents GD (Soman), VX and HD (Distilled Mustard) by two independent laboratories: Battelle Memorial Institute (Battelle), Columbus, OH; and the United States Soldier and Biological Chemical Command (SBC-COM), Edgewood, MD. All studies were conducted using controlled protocols at ambient room-conditions (temperature, pressure and humidity). The agent was placed on a glass surface and FAST-ACT was applied. Within 90 seconds FAST-ACT was validated to remove over 99.9% of HD and GD; and over 99.6% (detection limit) of VX from the surface (as determined by surface extraction followed by GC-MS analysis). Upon contact with FAST-ACT, the agent was quickly adsorbed and then destroyed. The destruction was confirmed by changes in the NMR spectra (SBCCOM) and by inability to extract the agent from the powder (Battelle). In 10 minutes 99% of GD and over 99.9% of VX is destroyed, while in about 60 minutes 70–80% of HD is destroyed.

## Safety of NanoActive Materials

Considering the high chemical reactivity of nanocrystalline metal oxides, a question to pose is, how safe are humans or animals if exposed to these materials? NanoScale has conducted rigorous toxicity testings at independent laboratories studying the oral, dermal, pulmonary and ocular effects of NanoActive metal oxides. The testings have revealed that there are no

safety-hazards associated with the nano nature of these materials. Dermal LD<sub>50</sub> (rabbit) was > 2 g/kg and oral LD<sub>50</sub> (rabbit) was > 5 g/kg. The formulation has also been tested for inhalation-toxicity and proven to be non-toxic to rats.

In addition, it was determined that in excess of 99.9% of the particles are captured by standard NIOSH particle filters (Flat media, Model 200 Series, N95 NIOSH, 30981J and Pleated filter with flat media, NIOSH Pro-Tech respirator, PN G100H404 OVIP-100). The non-toxic behavior of these particles in the inhalation testings, as well as the high removal efficiency can be explained by the formation of weak aggregates of nanomaterials. The nanocrystalline metal oxides manufactured at NanoScale aggregate into micron-sized particles due to their high surface reactivity. Micron-sized particles do not penetrate into the alveoli, but are stopped in the bronchia. NanoScale's products utilized for environmental applications are made from inherently non-toxic materials (magnesium oxide, calcium oxide, titanium dioxide, aluminum oxide) and possess higher solubility than their non-nano counterparts. Therefore, even if introduced into a human or animal body, they will dissolve and be expelled. Overall, the nanocrystalline materials produced at NanoScale were found to be no more toxic than the respective commercially available metal oxides.<sup>42</sup>

## Conclusions

Nanocrystalline metal oxides are highly effective adsorbents towards a broad range of environmental contaminants ranging from acids, chlorinated hydrocarbons, organophosphorus and organosulfur compounds to chemical warfare agents. These materials do not merely adsorb, but actually destroy many chemical hazards by converting them to much safer byproducts under a broad range of temperatures. Metal oxides produced by NanoScale were proven to be no more toxic than their non-nano commercial counterparts and continue to be a great choice for abating environmental pollutants.

## References

1. L. Interrante and M. Hampden-Smith (eds.), *Chemistry of Advanced Materials*, Chap. 7 (Wiley-VCH, 1998), pp. 271–327.
2. K. J. Klabunde, J. V. Stark, O. Koper, C. Mohs, D. G. Park, S. Decker, Y. Jiang, I. Lagadic and D. Zhang, *J. Physical Chemistry B* **100**, 12142–12153 (1996).
3. A. Khaleel, P. N. Kapoor and K. J. Klabunde, *NanoStruct. Materials.* **11**, 459–468 (1999); E. Lucas and K. J. Klabunde, *NanoStruct. Materials.* **12**,

- 179–182 (1999); O. Koper and K. J. Klabunde, U. S. Patent 6, 057, 488; May 2 (2000).
4. O. Koper, K. J. Klabunde, L. S. Martin, K. B. Knappenberger, L. L. Hladky, Decker P. Shawn, U.S. Patent 6, 653, 519; November 25 (2003).
  5. K. J. Klabunde, U.S. Patent 5,990,373; November 23 (1999).
  6. S. Rajagopalan, O. Koper, S. Decker and K. J. Klabunde, *Chem. Eur. J.* **8**, 2602 (2002).
  7. G. W. Wagner, P. W. Bartram, O. Koper and K. J. Klabunde, *J. Phys. Chem. B* **103**, 3225 (1999).
  8. G. W. Wagner, O. B. Koper, E. Lucas, S. Decker and K. J. Klabunde, *J. Phys. Chem. B* **104**, 5118 (2000).
  9. G. W. Wagner, L. R. Procell, R. J. O'Connor, S. Munavalli, C. L. Carnes, P. N. Kapoor and K. J. Klabunde, *J. Am Chem. Soc.* **123**, 1636 (2001).
  10. S. Decker, J. Klabunde, A. Khaleel and K. J. Klabunde, *Enviro. Sci. Technol.* **36**, 762–768 (2002).
  11. O. Koper, Y. X. Li and K. J. Klabunde, *Chem. Mater.* **5**, 500 (1993).
  12. O. Koper and K. J. Klabunde, *Nanophase Materials*, eds. G. C. Hadjipanayis and R. W. Siegel (Kluwer Academic Publishers, 1994), pp. 789–792.
  13. O. B. Koper, E. A. Wovchko, J. A. Glass Jr., J. T. Yates Jr. and K. J. Klabunde, *Langmuir* **11**, 2054–2059 (1995).
  14. O. Koper, I. Lagadic and K. J. Klabunde, *Chem. Mater.* **9**, 838–848 (1997).
  15. O. Koper and K. J. Klabunde, *Chem. Mater.* **9**, 2481–2485 (1997).
  16. R. J. Hedge and M. A. Barteau, *J. Catal.* **120**, 387–400 (1989).
  17. Y. X. Li, H. Li and K. J. Klabunde, *Nanophase Materials*, eds. G. C. Hadjipanayis and R. W. Siegel (Kluwer Academic Publishers, 1994), pp. 793–796.
  18. Y. X. Li, H. Li and K. J. Klabunde, *Environ. Sci. Technol.* **28**, 1248–1253 (1994).
  19. P. D. Hooker and K. J. Klabunde, *Environ. Sci. Technol.* **28**, 1243–1247 (1994).
  20. K. J. Klabunde, A. Khaleel and D. Park, *High Temp. Mater. Sci.* **33**, 99–106 (1995).
  21. A. Khaleel and K. J. Klabunde, *Nanophase Materials*, eds. G. C. Hadjipanayis and R. W. Siegel (Kluwer Academic Publishers, 1994), pp. 785–788.
  22. H. J. Kim, J. Kang, D. G. Park, H. J. Kweon and K. J. Klabunde, *Bull. Korean Chem. Soc.* **18**, 831–840 (1997).
  23. K. J. Klabunde, A. Khaleel and D. Park, *High Temperatures and Material Science*, **33**, 99–106 (1995).
  24. S. Decker and K. J. Klabunde, *J. Amer. Chem. Soc.* **118**, 12465–12466 (1996).
  25. Y. Jiang, S. Decker, C. Mohs and K. J. Klabunde, *J. Catal.* **180**, 24–35 (1998).
  26. S. Decker, I. Lagadic, K. J. Klabunde, J. Moscovici and A. Michalowicz, *Chem. Mater.* **10**, 674–678 (1998).
  27. Y. Jiang, S. Decker, C. Mohs and K. J. Klabunde, *J. Catalysis.* **180**, 24–35 (1998).
  28. I. N. Martyanov and K. J. Klabunde, *J. Catal.* **224**, 340–346 (2004).

29. Y. X. Li and K. J. Klabunde, *Langmuir*, **7**, 1388–1393 (1991).
30. Y. X. Li, J. R. Schulp and K. J. Klabunde, *Langmuir*, **7**, 1394–1399 (1991).
31. Y. X. Li, O. Koper, M. Atteya and K. J. Klabunde, *Chem. Mater.* **4**, 323–330 (1992).
32. M. K. Templeton and W. H. Weinberg, *J. Am. Chem. Soc.* **107**, 774–779 (1985).
33. Y. X. Li and K. J. Klabunde, *Langmuir*, **7**, 1388–1393 (1991).
34. S. T. Lin and K. J. Klabunde, *Langmuir* **1**, 600–605 (1985).
35. E. Lucas, S. Decker, A. Khaleel, A. Seitz, S. Fultz, A. Ponce, W. Li, C. Carnes and K. J. Klabunde, *Chem. Eur. J.* **7**, 2505–2510 (2001).
36. K. J. Klabunde, J. V. Stark, O. B. Koper, C. Mohs, D. G. Park, S. Decker, Y. Jiang, I. Lagadic and D. Zhang, *J. Phys. Chem.* **100**, 12142 (1996).
37. J. V. Stark and K. J. Klabunde, *Chem. Mater.* **8**, 1913–1918 (1996).
38. C. L. Carnes, J. Stipp, K. J. Klabunde and J. Bonevich, *Langmuir*, **18**, 1352–1359 (2002).
39. C. L. Carnes and K. J. Klabunde, *Chem. Mater.* **14**, 1806 (2002).
40. G. M. Medine, V. Zaikovskii and K. J. Klabunde, *J. Mater. Chem.* **14**, 757–763 (2004).
41. C. L. Carnes, P. N. Kapoor, K. J. Klabunde and J. Bonevich, *Chem. Mater.* **14**, 2922–2929 (2002).
42. USCHPPM Reports: 85-XC-01BN-03; 85-XC-5302-01; 85-XC-5302-03; 85-XC-03GG-11-05-01-02c; 85-XC-03GG-05; 85-XC-03GG-10-02-09-03. (Publication in preparation)